J Mater Sci: Mater Electron (2012) 23:1898–1904
DOI 10.1007/s10854-012-0681-1

Effect of substrate temperature on structural, morphological and optical properties of crystalline titanium dioxide films prepared by DC reactive magnetron sputtering

R. Ananthakumar · B. Subramanian · S. Yugeswaran · M. Jayachandran

Received: 19 October 2011 / Accepted: 2 March 2012 / Published online: 21 March 2012

Abstract Titanium dioxide (TiO_2) thin films have been deposited with various substrate temperatures by dc reactive magnetron sputtering method onto glass substrate. The effects of substrate temperature on the crystallization behavior and optical properties of the films have been studied. Chemical composition of the films was investigated by X-ray photoelectron spectroscopy (XPS). X-ray diffraction (XRD) analysis of the films revealed that they have polycrystalline tetragonal structure with strong (101) texture. The surface morphological study revealed the crystalline nature of the films at higher substrate temperatures. The TiO_2 films show the main bands in the range 400–700 cm^{-1}, which are attributed to Ti–O stretching and Ti–O–Ti bridging. The transmittance spectra of the TiO_2 thin film measured with various substrate temperatures ranged from 75 to 90 % in the visible light region. The optical band gap values of the films are increasing from 3.44 to 4.0 eV at growth temperature from 100 to 400 °C. The structural and optical properties of the films improved with the increase in the deposition temperature.

R. Ananthakumar · B. Subramanian (✉) · M. Jayachandran
Electrochemical Materials Science Division, CSIR, Central Electrochemical Research Institute, Karaikudi 630 006, India
e-mail: subramanianb3@gmail.com

R. Ananthakumar
Nanomaterials and System Lab, Department of Mechanical System Engineering, Jeju National University, Jeju 690-756, Republic of Korea

B. Subramanian · S. Yugeswaran
Joining and Welding Research Institute, Osaka University, Osaka 567-0047, Japan

1 Introduction

In the recent years nanostructure semiconductor materials have been the prime focus of scientific research due to their unusual optical, chemical [1], photo electrochemical and electronic properties [2, 3]. Therein titanium dioxide is one of the extensively used transition-metal oxide materials owing to its various important applications in self-cleaning [4], photocatalysis [5], environmental cleanup [6], dye-sensitized solar cells [7, 8], gas sensors [9], optical coatings [10] and purification of air and toxic gases because of its excellent chemical stability, photocatalytic decomposition of organics and contaminants, mechanical hardness, optical transmittance with high refractive index and strong redox ability [11]. Furthermore, the hydrophilic coating (0° water contact angle) has emerged as a new and very attractive application of TiO_2 [12, 13]. Since, the TiO_2 films exhibit heavy amphiphilc properties under ultraviolet (UV) light irradiation and are transparent in nature, it can be used in various kinds of applications such as self-cleaning and as anti-fogging materials in motor cars, buildings and household glazing [13].

Recently, the photocatalytic activity of TiO_2 has attracted great attention and has become a major focus of research. Performance of TiO_2 thin films as a photocatalyst, for solar cells or gas sensor depends not only on its energy band structure but, to a great extent, on its crystal structure, size and morphology [14]. In addition, process and processing conditions under which thin films are synthesized lead to significant variations in their morphology, crystallite size and optical properties [14].

Titanium dioxide exists in three crystalline phase: Brookite in orthorhombic structure and Rutile and Anatase in tetragonal structure. Both rutile and anatase show photocatalytic activities, while the anatase is generally more

active in photocatalysis a rutile. Such difference is attributed to the lower band-gap of the anatase than that of the rutile. The anatase TiO_2 is found to exhibit interesting properties, which make it a promising material for gas sensors, solar cells and dielectric in semiconducting FETs [15]. The anatase phase has been reported to develop at temperatures below 800 °C, which at higher temperatures transforms to the more stable rutile phase [14].

The preparation of TiO_2 films has been carried out by using a number of techniques such as thermal evaporation [16], pulsed laser deposition [17], ion-assisted deposition, anodic oxidation of titanium, chemical vapor deposition, plasma enhanced chemical vapor deposition, electron beam evaporation, dc and rf reactive sputtering methods [18]. Among the various methods to immobilize TiO_2 thin film, sputtering methods have attracted great attention because of some advantages, such as higher and easily controlled sputtering speed, high quality and uniform films and convenient manipulation, make the deposition process like reactive magnetron sputtering are currently used to produce high purity oxide film for applications in various advanced technologies. Apart from the benefits noted above it is attractive for the film fabrication technique to keep the substrate at low temperature during the sputtering deposition course, which allows the material with low melting point to the used as substrate. Furthermore sputtering deposition should be one of the most promising techniques for the large-area uniform coating with high packing density and strong adhesion. The use of a reactive magnetron sputtering provides more benefit in controlling the structure, composition and photocatalytic properties of TiO_2 films due to the ease of adjusting various deposition conditions [19]. It has been previously observed that changing of substrate temperature has a strong effect on the final crystalline phase of the TiO_2 thin film, prepared on different substrates [20].

Hossain et al. [21] have reported that the TiO_2 films are deposited at different substrate temperatures for evaluating an ideal substrate temperature, which leads to the favorable structural and morphological properties of the TiO_2 films for maximizing the photovoltaic performances. Luca et al. [22] have prepared TiO_2 thin films by pulsed laser deposition method and the characteristics of the investigated thin films are interpreted in terms of amorphous-crystalline phase transitions and the role of oxygen defects. Musil et al. [23] observed substantial variation of crystallinity and crystalline phase with small variation in substrate temperature. Sankar et al. [24] discussed about the phase transformation from amorphous to anatase and then to rutile TiO_2 with annealing temperature. In this paper, we optimized the two sputtering parameters, sputtering pressure and Ar to O_2 gas ratio and investigated the influence of substrate temperature on structural, microstructural and optical properties of titanium dioxide thin films, deposited by dc reactive magnetron sputtering for photocatalytic applications.

2 Experimental methods

TiO_2 thin films were deposited on well cleaned glass substrates using a dc magnetron sputter deposition unit. The base vacuum of the chamber was below 1×10^{-6} mbar for different substrate temperatures. Highly pure argon was fed into the vacuum chamber for the plasma generation. The substrates were etched for 5 min at a dc power of 50 W and an argon pressure of 10 min for (1.33 Pa). The deposition parameters for TiO_2 sputtering are summarized in Table 1.

The chemical nature of the outermost part of TiO_2 films was obtained by X-ray photoelectron spectroscopy (XPS) using Multilab 2000. The crystal structure and preferred orientation of the TiO_2 coatings were examined by XRD using PANalytical-3040 X'pert pro diffractometer operated at 40 kV and 30 mA with CuKα (1.5414 Å) radiation. Fourier transform infrared (FTIR) studies were conducted with Perkin Elmer system. The surface morphology of the coating was characterized by scanning electron microscopy (SEM) using a Hitachi S 3000H microscope. Optical measurements were carried out for the TiO_2 coated glass substrate using a HITACHI U-3400 spectrophotometer in the wavelength range of 300–850 nm. The photoluminescence (PL) measurements were made using a Cary Eclipse fluorescence spectrophotometer (VARIAN) employing a PbS photodetector and a 150 W Xe arc discharge lamp as the excitation light source.

3 Results and discussion

3.1 Composition and structural analysis

XPS is a useful technique in elucidating surface chemistry, which is responsible for the chemical and electrochemical characteristics of thin film. Figure 1a shows the survey spectra of TiO_2 film coated glass substrates and exhibited

Table 1 Deposition parameters for TiO_2 reactive sputtering

Objects	Specification
Target (2″Dia)	Ti (99.9 %)
Substrate	Glass
Target to substrate distance	60 mm
Ultimate vacuum	1×10^{-6} mbar
Operating vacuum	2×10^{-3} mbar
Sputtering gas (Ar:O_2)	2:1
Power	150 Watt
Substrate temperature	100 °–400 °C

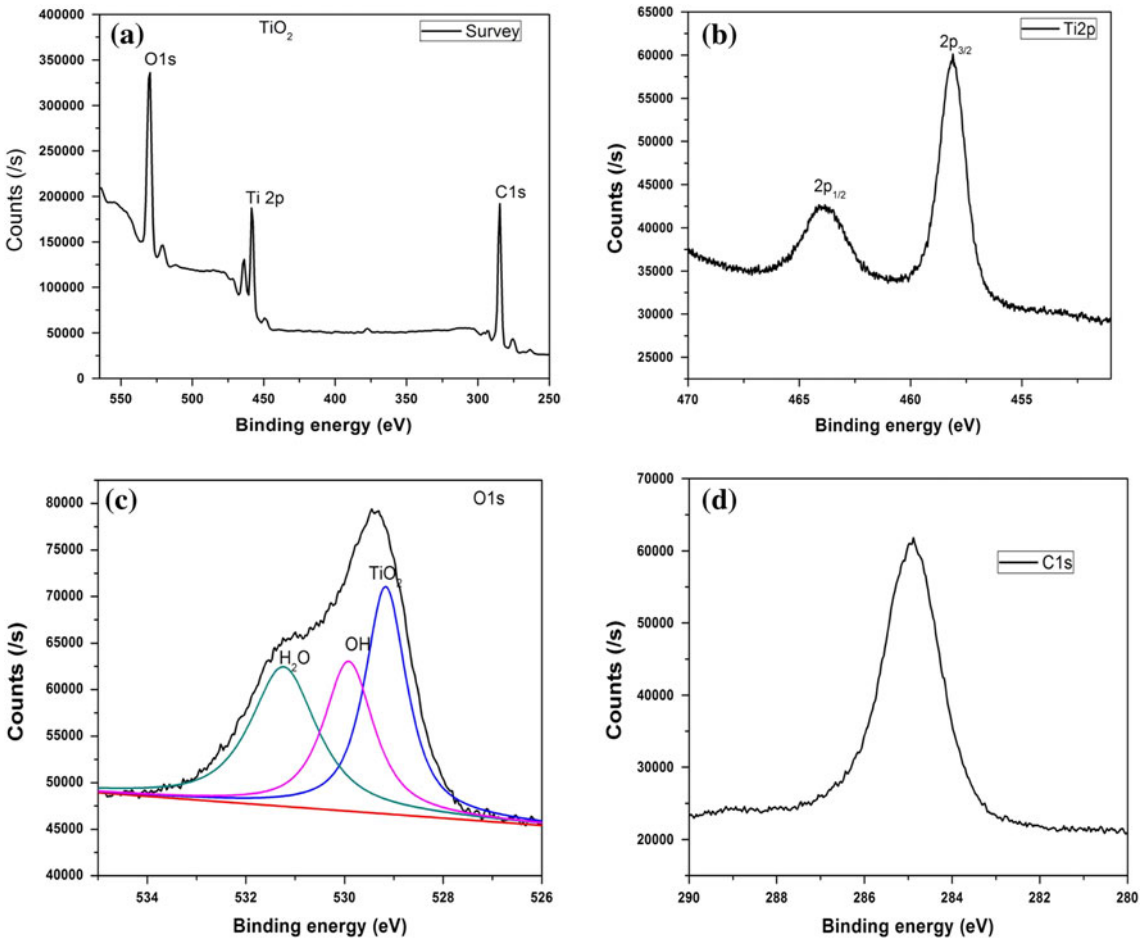

Fig. 1 XPS spectra of Ti 2p and O 1s on the TiO_2 film deposited on glass substrate **a** Survey **b** Ti 2p **c** O 1s and **d** C 1s spectra

the characteristics peaks Ti 2p, O 1s, and C 1s with the corresponding binding energies 458.7, 530.1 and 285.2 eV [25] respectively. Ti 2p spectrum of the film and binding energies of Ti $2p_{3/2}$ and Ti $2p_{1/2}$ are observed at 458.1 (Fig. 1b) and 463.8 eV, respectively [26], which are assigned to the Ti^{4+} (TiO_2), with a peak separation of 5.7 eV between peaks. The O 1s spectra of TiO_2 film can be resolved into three peaks as seen in Fig. 1c at 529.1, 530.0 and 531.2 eV [27]. They are assigned to lattice O_2, hydroxyl groups and adsorbed water or organic matters, respectively. Figure 1d shows the C 1s spectra with the corresponding binding energy of 285.2 eV. The element C in the film is attributed to the residual carbon.

X-ray diffraction patterns of TiO_2 films prepared on glass substrates by DC-magnetron sputtering at various substrate temperatures are shown in Fig. 2. Three well defined peaks, identified as anatase A (101), A (004) and A (105) TiO_2 lines, are clearly observed, indicating the polycrystalline tetragonal structure of TiO_2 films at 400 °C. The films have random growth orientations. The random growth orientation is understandable because of the amorphous nature of the substrates. It is observed that the intensity of the (101) peak increased with increasing substrate temperature and reached a maximum at 200 °C. As the temperature was further increased above 200 °C, the intensity of the (101) peak decreased and the (004) peak appeared. This means that since the surface mobility of the sputtered particles increased with increasing substrate temperature, the closely packed (101) plane having the smallest surface energy grew and the degree of preferred orientation was increased by the enhancement of the sticking force between the particles and substrate. In addition, the (004) peak was observed at substrate temperatures above 300 °C, this means that the appearance of the (004) peak plays a major role in decreasing the c-axis orientation. The other reason may be increase in particle size with increasing temperature as can be estimated from diffraction patterns. The diffraction peaks of rutile (110), (200), and (211) appear when substrate temperature is at 500 °C. With further increase in annealing temperature, it is observed that intensity of diffraction peaks of anatase decreases and that of rutile increases. The results clearly

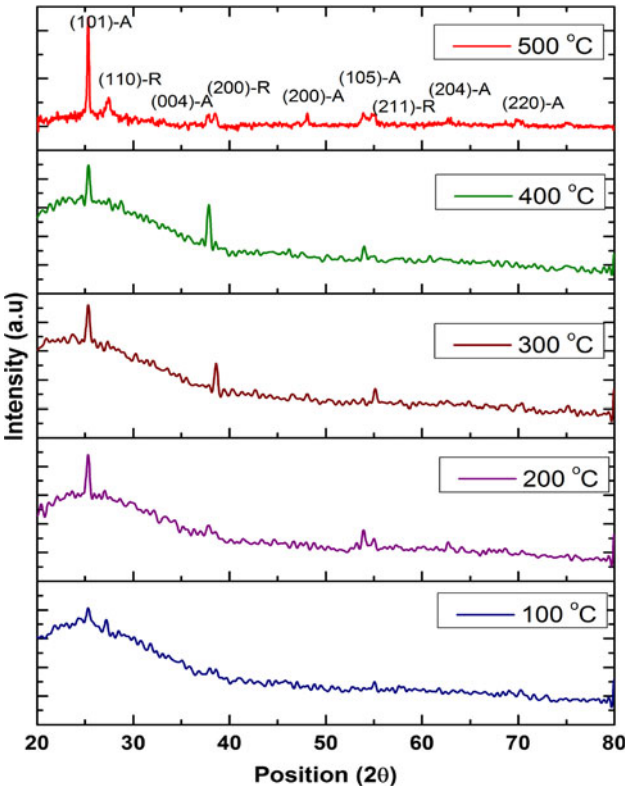

Fig. 2 XRD pattern for TiO_2 thin films at different substrate temperatures

indicate the transformation from amorphous to anatase and then to rutile phase with increase in annealing temperature and is in good agreement with the prior reports regarding the phase evolution in TiO_2 [24].

The average crystallite sizes of the films deposited at different substrate temperatures have been calculated using the Scherrer's formula [28]

$$D = \frac{0.94\lambda}{\beta \cos e} \quad (1)$$

where λ, θ and β are X-ray wavelength, the Bragg's diffraction angle and the full width at half maxima (FWHM) of the peak corresponding to the "θ" value, respectively. The crystallite size is found to increase from 12 to 68 nm as the growth temperature is increased from 100 to 400 °C.

FTIR is also a useful technique to obtain the structural information and the chemical state of the TiO_2 film. The TiO_2 films show (Fig. 3) the main bands in the range 400–700 cm^{-1}, which are attributed to Ti–O stretching and Ti–O–Ti bridging. The bands in the regions of 1,000–1,300 cm^{-1}, observed for non-sensitized TiO_2, were attributed to stretching and vibrations of the Ti–O–Ti group, indicating the formation of the inorganic matrix [29]. The broad bands at 2,800–3,800 cm^{-1} are assigned to the O–H vibration of water molecules [30]. This absorption

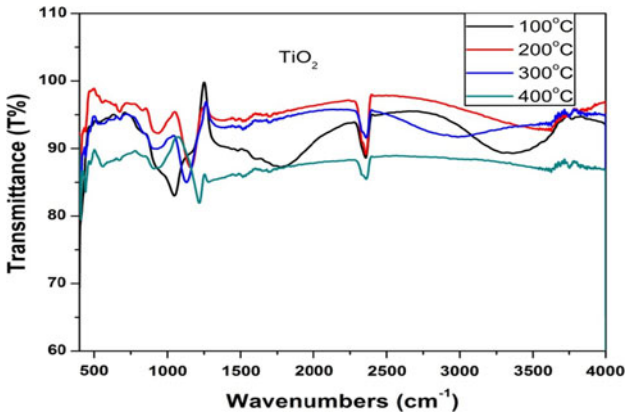

Fig. 3 FTIR spectra of TiO_2 thin films for different substrate temperatures

band is caused by the bending vibration of coordinated H_2O as well as Ti–OH.

3.2 Morphological properties

Effects of substrate temperature on the surface morphology of the TiO_2 thin films were investigated by SEM. Figure 4 shows an SEM image of the TiO_2 film deposited on glass substrate at 100 °–400 °C. The surface image of the film prepared at lower substrate temperature (100 °C) (Fig. 4a) are having uniform surface with low crystallinity behavior. As the substrate temperature increases from 200 ° to 400 °C (Fig. 4b–d), the surface becomes smooth and dense indicating an improvement in the crystallinity. They showed many, well shaped nano particle grains homogeneously distributed all over substrate surfaces. It is because the heat emerges immediately at higher temperature to the films from coalescence stage to the perfect growth nature and all the evaporated particles get well shape. This result agrees well with the XRD analysis.

3.3 Optical properties

Figure 5 shows the absorption spectra of the TiO_2 thin films. The absorption spectra were obtained by using a reference glass substrate. The ripples in the spectra results from the interference of the light since they showed waveform which is a characteristic of the interference light [31]. It can be noticed from the Fig. 5 that the absorption edge exhibits a slight blue shift. It is a reflection of the quantum size effect [32]. The energy shift in the band gap as a function of particle size can be predicted by three dimensional confinement model based on the effective mass approximation [33].

Optical transmission spectra of TiO_2 films deposited at different deposition temperatures are shown in Fig. 6. In principle, $T(\lambda)$ should be depending on the stoichiometry,

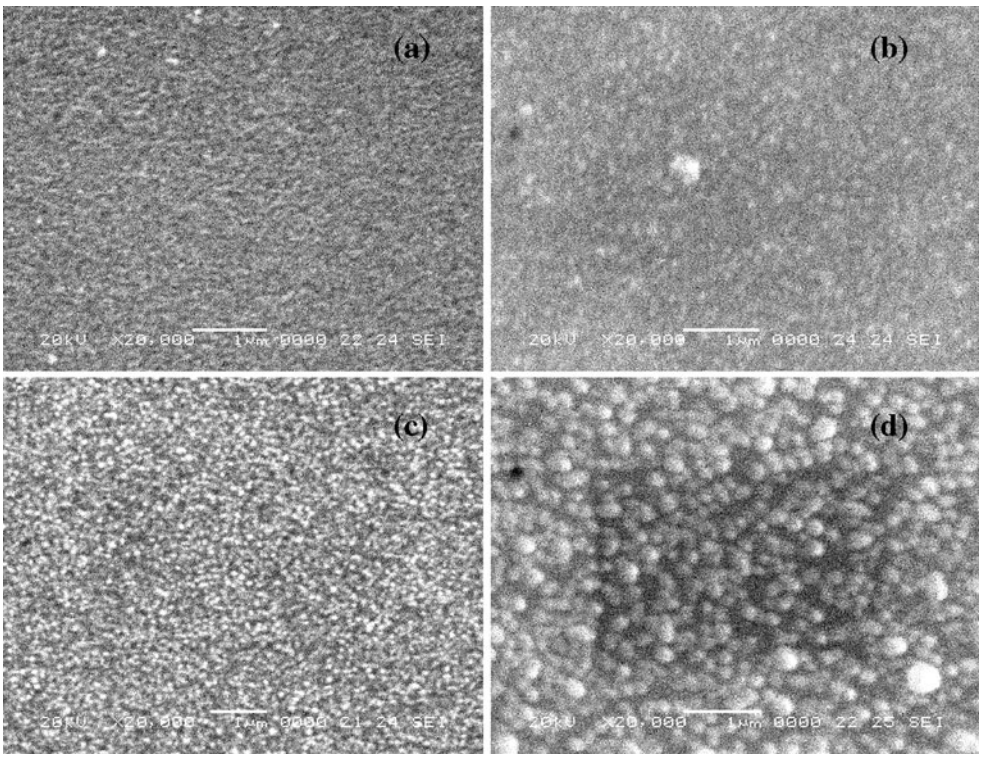

Fig. 4 SEM micrographs of TiO_2 thin films grown at different temperatures: **a** 100 °C, **b** 200 °C, **c** 300 °C and **d** 400 °C

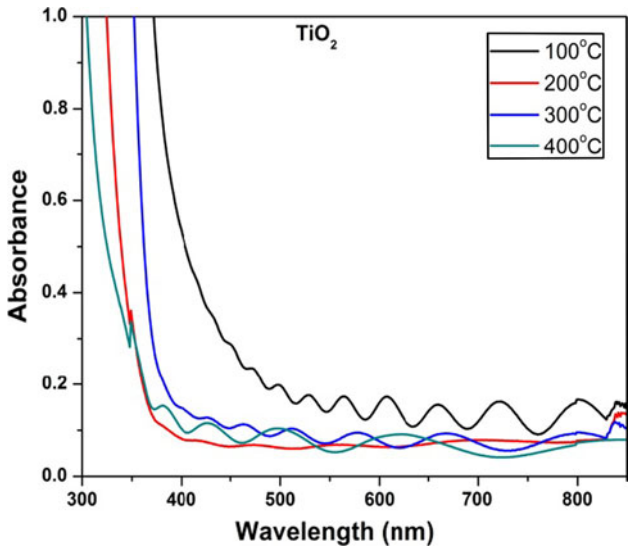

Fig. 5 Absorbance spectra of TiO_2 thin films for different substrate temperatures

crystallinity, and thickness of the film, which are controlled by the deposition process. It is found that the average transmittance of all as-deposited films is above 60 % in the visible region. This indicates that TiO_2 film can be used as a window material in solar cells. This implies that the film has good optical quality. The optical transmission of TiO_2 films as clearly seen in the visible wavelength region is increasing with deposition temperature. Interference fringes were observed in all cases. The increase in optical transmittance with the rise of deposition temperature can be attributed to the increase of structural homogeneity and the decrease of defects.

The optical band gap of TiO_2 film can be determined from the absorption spectra. The absorption coefficient, 'α' is related to the optical band gap Eg by the relation [34],

$$\alpha h\upsilon = B(h\upsilon - Eg)^n \quad (2)$$

where h is Plank's constant, υ is the frequency of the radiation, B is a constant which depends on the nature of transition and n is a number which can take the values 1/2, 3/2, 2 or more depending on whether the transition is direct-allowed, direct-forbidden, indirect-allowed or indirect-forbidden. In the present case for the TiO_2 thin films, the plots of $(ah\upsilon)^2$ versus $h\upsilon$ (Fig. 7) show a linear portion indicating that the relation in Eq. (2) holds good for TiO_2 films if $n = 1/2$. This means that the optical transitions are direct transitions. The direct band gap (Eg) is determined by extrapolating the straight-line portion of the plot to the energy axis. The intercept on energy axis gives the value of band gap energy Eg (Fig. 7) for all the samples and the values lie in the range of 3.44–4.00 eV respectively. The results denote that a higher optical band gap can be obtained by increasing the substrate temperature. Yang et al. [35] reported that the direct band gap for TiO_2 films

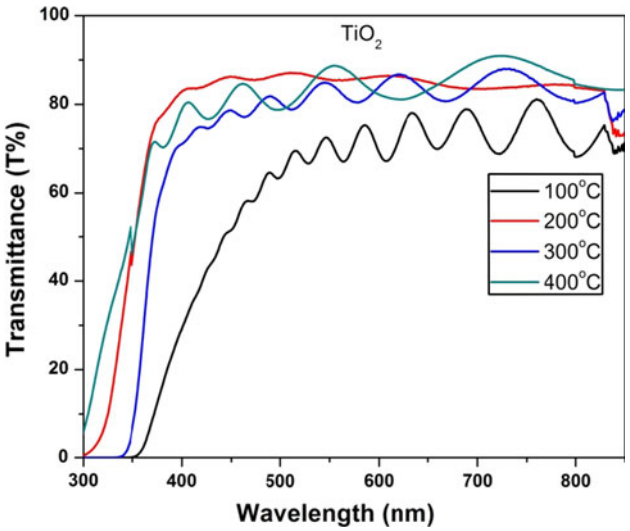

Fig. 6 Transmittance spectra of TiO_2 thin films for different substrate temperatures

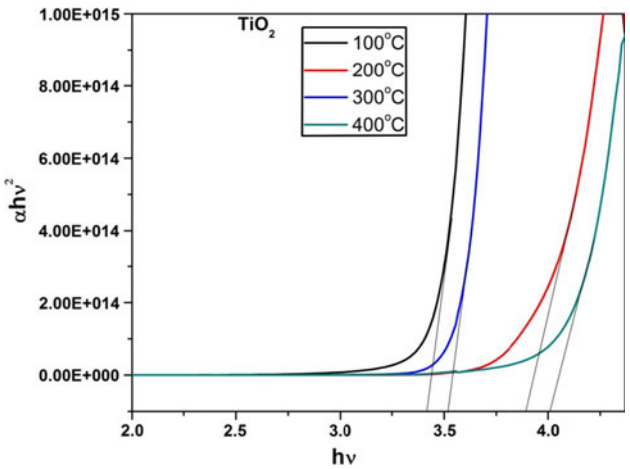

Fig. 7 Variation of hν with $\alpha h\nu^2$ for TiO_2 thin films for different substrate temperature

increased from 3.81 to 3.92 eV as the substrate temperature was increased from 50 to 300 °C. The allowed direct transitions have been previously found for different TiO_2 films and the direct optical band gap, with Eg values ranging from 3.77 to 3.85 eV have been reported [36]. It can be seen from the figure that the band gap increases with the increase of the substrate temperature. The optical band gap of TiO_2 thin film is obviously affected by the defects and the crystallinity. From Fig. 7 and based on the results of XRD and SEM analysis, it is apparent that the optical band gap increases with the decrease in defects and with the increase in grain size. This can be explained by the fact that free electrons are trapped in the defects and in the grain boundaries. The density of defects decreases with the increase in substrate temperature and the density of grain boundaries decreases when the grain size increases at

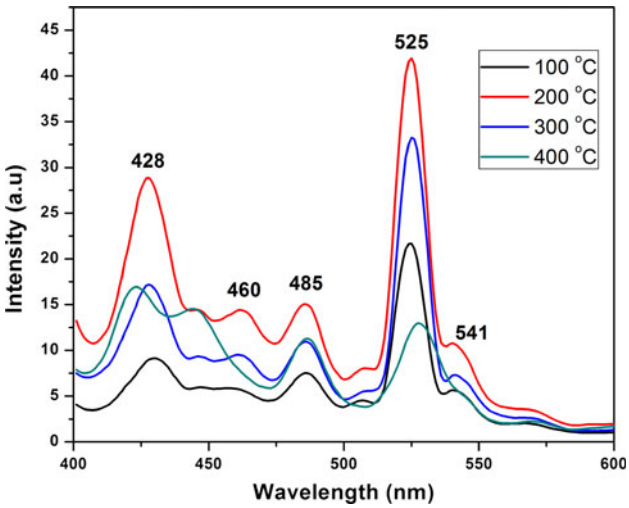

Fig. 8 Photoluminescence spectra of TiO_2 thin films for different substrate temperature

higher substrate temperature. As a result, fewer carriers are trapped there leading to a higher amount of free carriers, which means higher conductivity [37].

Figure 8 shows the PL spectrum of TiO_2 thin films deposited at different substrate temperatures under the excitation with a wavelength of 255 nm. The PL spectra emitted five peaks located at 428, 460, 485, 525 and 541 nm which are due to anatase phase of TiO_2 thin films [38]. All these peaks were also observed for the rutile TiO_2 films prepared at higher temperature, but with considerably decreased PL peak intensities. The PL spectra of anatase and rutile TiO_2 films have been interpreted as emissions from self-trapped excitons and free excitons, respectively [39]. In the present case, a well defined peak at 525 nm in the spectra appears only for the anatase phase. The peaks showed slight shift into lower wavelength at higher temperatures. Such a shift may be attributed to donor–acceptor band transition, where excess Ti acts as donor while some impurity or defects present at the surface and interface of the film acts as acceptor. In the PL spectra the peaks are found to be broadening out with increase in substrate temperature and the broadening of peaks may be attributed to the higher concentration of defects.

4 Conclusions

Titanium dioxide thin films were deposited by dc reactive magnetron sputtering with substrate temperatures varying from 100 to 400 °C. The effect of substrate temperature of the TiO_2 thin films on the structural and optical properties was investigated. XPS analysis has shown that the binding energies of Ti 2p, O 1s and C 1s are 458.7, 530.1 and 285.2 eV, respectively. With the increase in substrate

temperature, it was observed that there is a corresponding increase in grain growth and crystallinity of TiO_2 thin films deposited on glass substrates. The XRD spectra indicated that the films are polycrystalline tetragonal structure with preferential orientation of (101) plane. The existence of Ti–O bands was confirmed from IR spectra. The transmittance spectra also confirmed that the deposition temperature has a significant effect on the transparency of the thin films. The highest transparency over the visible wavelength region of spectra was obtained at the deposition temperature of 400 °C. The allowed direct band gap at the deposition temperature ranging from 100 to 400 °C was estimated to be in the range from 3.44 to 4.00 eV. Good optical quality of these films was observed from PL studies. In the PL spectra the peaks are found to broaden out with increase in substrate temperature and the broadening of peaks can be attributed to high concentration of defects.

Acknowledgment One of the authors (B.S) thanks the Department of Science & Technology, New Delhi, for a research grant under SERC scheme No SR/S1/PC/31/2008.

References

1. A. Kumar, S. Mandal, P.R. Selvakannan, R. Pasricha, A.B. Mandale, M. Sastry, Langmuir **19**, 6277 (2003)
2. N. Chandrasekharan, P.V. Kamat, J. Phys. Chem. B **104**, 10851 (2000)
3. G. Peto, G.L. Molnar, Z. Paszti, O. Geszti, A. Beck, L. Guczi, Mater. Sci. Eng. C **19**, 95 (2002)
4. W. Zhang, Y. Li, S. Zhu, F. Wang, Surf. Coat. Technol. **182**, 192 (2004)
5. Y. Matsumoto, Y. Ishikawa, M. Nishida, S. Ii, J. Phys. Chem. B **104**, 4204 (2000)
6. M. Andersson, L.O. Sterlund, S. Ljungstrom, A. Palmqvist, J. Phys. Chem. B **106**, 10674 (2002)
7. G. Benk, P. Myllyperki, J. Pan, A.P. Yartsev, V. Sundstrom, J. Am. Chem. Soc. **125**(5), 1118 (2003)
8. S. Karuppuchamy, K. Nonomura, T. Yoshida, T. Sugiura, H. Minoura, Solid State Ionics **151**, 19 (2002)
9. A. Rothschild, A. Levakov, Y. Shapira, N. Ashkenasy, Y. Komem, Surf. Sci. **532**, 456 (2003)
10. T. Watanabe, A. Nakajima, R. Wang, M. Minabe, S. Koizumi, A. Fujishima, K. Hashimoto, Thin Solid Films **351**, 260 (1999)
11. S. Takeda, S. Suzuki, H. Odaka, H. Hosono, Thin Solid Films **392**, 338 (2001)
12. R. Wang, K. Hashimoto, A. Fujishima, M. Chikuni, E. Kojima, A. Kitamura, M. Shimohigoshi, T. Watanabe, Adv. Mater. **10**, 135 (1998)
13. N. Sakai, A. Fujishima, T. Watanabe, K. Hashimoto, J. Phys. Chem. B **105**(15), 3023 (2001)
14. R. Mechiakh, N. Ben Sedrine, R. Chtourou, Appl. Surf. Sci. **257**, 9103 (2011)
15. B. Karunagaran, K. Kim, D. Mangalaraj, J. Yi, S. Velumani, Sol. Energy Mater. Sol. Cells **88**, 199 (2005)
16. H.K. Pulker, G. Paesold, E. Ritter, Appl. Opt. **18**, 1969 (1979)
17. S. Sin-iti Kitazawa, Y. Choib, S. Yamamoto, Vacuum **74**(3–4), 637 (2004)
18. F. Meng, F. Lu, Vacuum **85**, 84 (2010)
19. S.K. Zheng, T.M. Wang, G. Xiang, C. Wang, Vacuum **62**, 361 (2001)
20. Y. Zhang, X. Ma, P. Chen, D. Yang, J. Cryst. Growth **300**, 551 (2007)
21. F. Hossain, T. Takahashi, J. Nanosci. Nanotechnol. **11**, 3222 (2011)
22. D. Lucaa, L.S. Hsu, J. Optoelect. Adv. Mater. **5**(4), 835 (2003)
23. S. Sankar, K.G. Gopchandran, Cryst. Res. Technol. **44**(9), 989 (2009)
24. J. Musil, D. Herman, J. Sicha, J. Vac. Sci. Technol. A **24**, 521 (2006)
25. R. Gouttebaron, D. Cornelissen, R. Snyders, J.P. Dauchot, M. Wautelet, M. Hecq, Surf. Interface Anal. **30**, 527 (2000)
26. Z. Lei, L. Jian-She, Trans. Nonferrous Met. Soc. China **17**, 772 (2007)
27. L.J. Meng, C.P. Moreira de Sa, M.P. Dos Santos, Thin Solid Films **239**, 117 (1994)
28. B. Subramanian, R. Ananthakumar, V.S. Vidhya, M. Jayachandran, Mater. Sci. Eng. B **176**(1), 1 (2011)
29. M.B. González, A. Wu, P.M. Vilarinho, Chem. Mater. **18**, 1737 (2006)
30. R. Zhang, L. Gao, Key Eng. Mater. **224–226**, 573 (2002)
31. D.C. Paine, T. Whistion, D. Janiac, R. Bersford, C.O. Yang, B. Lewis, J. Appl. Phys. **85**, 8445 (1999)
32. M. Anpo, T. Shima, S. Kodama, Y. Kubokawa, J. Phys. Chem. **91**, 4305 (1987)
33. A.L. Linsebigler, G.Q. Lu, J.T. Yates Jr, Chem. Rev. **95**, 735 (1995)
34. K.L. Chopra, S.R. Das, *Thin film solar cells* (Plenum press, New York, 1983)
35. C. Yang, H. Fan, Y. Xi, J. Chen, Z. Li, Appl. Surf. Sci. **254**, 2685 (2008)
36. M.R. Teresa, M. Viseu, C. Isabel, Vacuum **52**, 115 (1999)
37. H.R. Fallaha, M. Ghasemia, A. Hassanzadehb, H. Stekic, Mater. Res. Bull. **42**(3), 487 (2007)
38. W.F. Zhang, M.S. Zhang, Z. Yin, Q. Chen, Appl. Phys. B **70**, 261 (2000)
39. H. Tang, H. Berger, P.E. Schmid, F. Levy, Solid State Commun. **87**, 847 (1993)